Journal of Scientific & Industrial Research
Vol. 80, May 2021, pp. 391-397

Adsorption of Congo Red from Aqueous Solution using Doped Strontium Hexaferrite – Zero Valent Iron Nanocomposite: Kinetic, Isotherm, and Thermodynamic Studies

Shaghayegh Mehrjooyan, Mahmoud Reza Sohrabi* and Saeid Mortazavinik
Department of Chemistry, North Tehran Branch, Islamic Azad University, Tehran, Iran

Received 15 July 2020; revised 06 February 2021; accepted 24 April 2021

This study has dealt with synthesis of doped strontium hexaferrite / zero-valent iron nanocomposite ($SrFe_{12}O_{19}$/nZVI) and adsorption of Congo Red (CR) dye by the nanocomposite from aqueous solution was evaluated. The adsorbent was characterized using Fourier transform infrared spectroscopy (FT-IR), X-ray diffraction (XRD) analysis and Scanning Electron Microscopy (SEM). Optimization of experimental conditions such as pH, initial concentration of pollutant, adsorbent weight, contact time, and temperature was done. Maximum removal efficiency was achieved at pH of 8.5, initial concentration of CR=20 μg mL^{-1}, adsorbent weight of 0.12 g with 15 min contact time and 25ºC temperature. Langmuir isotherm with R^2=0.9959 seems to have best fit to the CR adsorption results. Also, kinetic studies revealed that adsorption of CR was fitted to the pseudo-second-order model with R^2=0.9969. In addition, thermodynamic parameters were evaluated.

Keywords: Adsorption, Congo Red, Isotherm, Kinetic, Strontium hexaferrite, Zero valent iron

Introduction

A huge volume of dye bearing wastewater is generated by various industries such as pharmaceutical, cosmetic, paper, plastics, rubber, leather, food, and textile industries every year.[1] Dyes are widely used in these industries and they are one of the major pollutants for aquatic environment.[2] Three important categories of dyes (i) anionic; (ii) cationic, as well as (iii) nonionic are mostly in use.[3] One of the anionic dye is Congo Red (CR).[4] It is released into aquatic environment during dyeing and finishing processes from various industries such as textile, printing, leather, pulp, paper, and cosmetic.[5,6] Conventional techniques are inefficient in treating the benzene and naphthalene rings that are present in CR.[7] This dye has several effects on human health, like an anaphylactic shock as well as irritation of skin, eye, and gastrointestinal tract. Also, it causes blood clots and respiratory problems.[8] Furthermore, it is a carcinogen and a mutation factor for human beings.[9,10] Hence, removing CR from wastewater before discharge into water resource is essential. Various techniques such as coagulation[11], flocculation[12], reverse osmosis[13], membrane separation[14], electrochemical treatment[15], photo-degradation[16], ozonation[17], advanced oxidation[18], and adsorption[19] are in use for removal of dyes from wastewater. Among these methods, the adsorption process is simple, easy to handle, inexpensive, and highly efficient.[20] Several adsorbents such as activated carbon[21], multi walled carbon nanotubes (MWCNTs)[22], zeolites[23], graphene oxide[24], nanoparticles (NPs)[25], nanocomposites[26], polymers[27], etc., have been widely used for the adsorption dyes. Strontium hexaferrite ($SrFe_{12}O_{19}$) has high permeability, excellent chemical stability, large magnetocrystalline anisotropy, as well as low conductive harms. So, it can be used in the permanent magnets, magneto-optic, microwave devices, and high-density recording media.[28,29] On the other hand, nano-zerovalent iron (nZVI) possesses high reactivity, large specific surface area, is inexpensive, and environmentally friendly. It has been used as a remediation agent in the environment.[30,31] The magnetic attraction of nZVI particles is responsible for their tendency to accumulate and diminish the reaction.[32] This problem has been solved by using supporter materials such as graphene[33], bentonite[34], and chitosan[35] etc. In the present study, doped strontium hexaferrite–zero valent iron nanocomposite ($SrFe_{12}O_{19}$/nZVI) was prepared to removal CR from aqueous media.

*Author for Correspondence
E-mail: Sohrabi.m46@yahoo.com

Materials and Methods

Materials

Iron(III) chloride, Sodium borohydride, Citric acid, Strontium nitrate, Chromium nitrate, Iron(III) nitrate, Ammonia, acetone, and Congo red were purchased with high purity from Merck.

Synthesis of Doped Chromium (Cr) Strontium Hexaferrite

Stoichiometric values of citric acid, iron(III) nitrate, strontium nitrate and chromium nitrate were dissolved in sufficient amount of distilled water. This solution was stirred at 60°C to become completely uniform. Then, the diluted ammonia solution was added till the pH of the solution reached 7. Afterward, this solution was heated at 80°C for 3 h to make a black viscose gel. By continuing the heat, the combustion was carried out. The obtained powder was heated in the furnace at 900°C for 3 h to form the M-type of strontium hexaferrite phase.[36]

Preparation of Zero-Valent Iron Nanoparticles

In a beaker 200 ml of distilled water was taken and stirred with a mechanical stirrer under nitrogen gas. Then, 2.0 g iron (III) chloride was added to this solution. Afterward, the other solution was prepared from dissolving 1 g sodium borohydride in distilled water and transferred into the burette. The second solution was slowly added to the first solution and reduction of iron (III) to zero iron was done. The solution below the burette was filtered by a vacuum pump. Finally, the precipitate was placed inside the desiccator to dry.

Preparation of Doped Strontium Hexaferrite-Zero Valent Iron NPs

Two grams of iron (III) chloride was dissolved and stirred in 300 ml distilled water under nitrogen gas. Then, 0.65 g of doped strontium hexaferrite was added. By adding sodium borohydride, reduction of Fe^{3+} was done. The resulting mixture was filtered by a vacuum pump. Ultimately, the obtained sediment, which consists of $SrFe_{12}O_{19}$/nZVI, was placed inside the desiccator to dry.

Characterization of Adsorbent

Samples were tested using FT-IR spectrophotometer (model NICOLET 8700, Thermo Scientific Co.,). UV-Vis double beam spectrophotometer equipped with 1.0 cm quartz cells (Bio-TEK model No.992) was used for spectrophotometric measurements. Analysis of the synthesized nanocomposite was studied by X-ray diffraction (Panalytical Co.,). The morphologies of the synthesized particles were analyzed by SEM (Philips XL 30, Netherlands). A digital Bante pH meter (model 930, China) was used to adjust the pH values of the solutions. Also, oven (Memmert, Germany) was utilized.

Preparation of Solutions

For this purpose, 10, 20, 30 ppm of Congo Red solutions were prepared and their absorption spectra were recorded by UV-Vis spectrophotometry. Among them, the solution of 30 ppm was appropriate and showed that λ_{max} of this color was 500.758 nm. In the next step, different experimental conditions were optimized for dye removal.

Results and Discussion

Characterization of Nanoadsorbent

The FTIR spectrum of $SrFe_{12}O_{19}$/nZVI is shown in Fig. 1(a). The absorption band in the region of 470 cm^{-1} and 540 cm^{-1} are assigned to the Fe-O vibrating bands. Fe is located in the octahedral and tetrahedral cavities between the O^{2-} in the $SrFe_{12}O_{19}$ network. The difference between these two absorption bands is due to the Fe-O bond length difference in octahedral and tetrahedral cavities. Wherever the bond length is more, the frequency of the stretching vibrations of the bond will be less. The FTIR spectrum of $SrFe_{12}O_{19}$/nZVI is demonstrated in Fig. 1(b). Zero-valent iron is bonded to hexaferrite and has produced magnetic gravity. So, peaks at 470 cm^{-1} and 540 cm^{-1} have been observed again, and the coupling magnetic zero-valent iron to hexaferrite does not change the location of the hexaferrite absorption bands. The SEM image of the doped strontium hexaferrite is indicated in Fig. 2(a). Hexaferrite bear independent hexagonal particles. Due to their magnetic nature, they are connected together in some areas. As shown in the figure, the particle surface is uniform. The SEM image of nanocomposite is illustrated Fig. 2(b). Zero-valent iron particles have been adsorbed on hexaferrite particles. Hexaferrite is surrounded by the iron NPs and covered them. The distribution of iron particles is uniform on the surface. The XRD spectrum of doped strontium hexaferrite as illustrated in Fig. 3(a) conforms to the crystalline structure of the M-type hexaferrite, and the obtained peaks in 2θ correspond with crystalline plates. The XRD spectrum of nanocomposite is represented in Fig. 3(b). Iron NPs

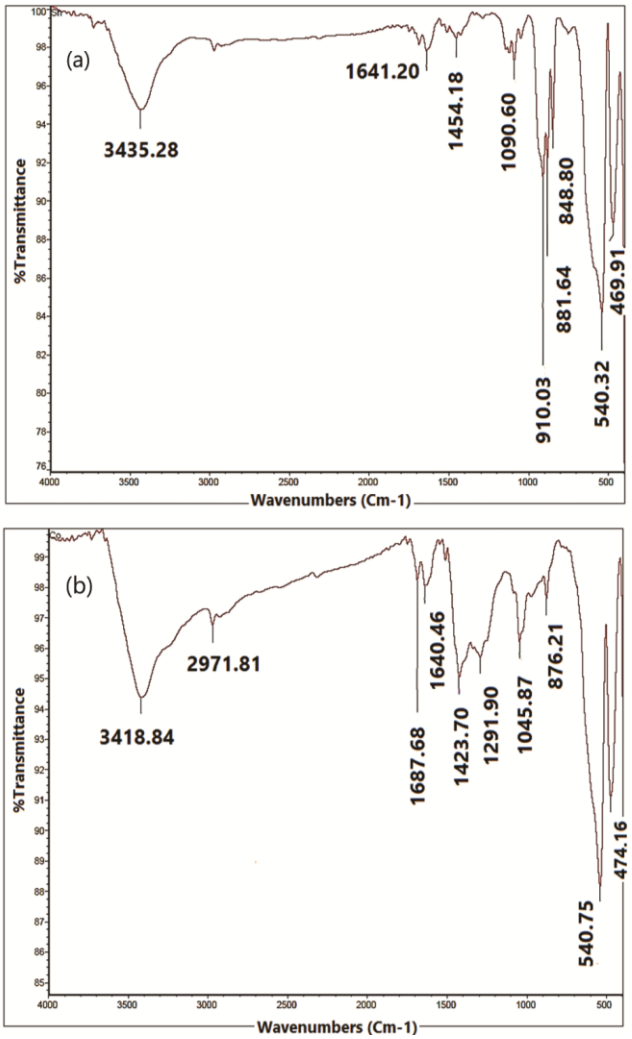

Fig. 1 — FTIR spectrum of (a) doped strontium hexaferrite and (b) nanocomposite

are adsorbed to hexaferrite particles due to magnetic gravity. These connections are physical and do not effect on the crystalline structure of the hexaferrite. Therefore, location of peaks in XRD pattern of the adsorbent is similar to the pure hexaferrite.

Effect of Adsorbent Dosage and Contact Time

For this purpose, 0.05, 0.1, and 0.12 g of nanocomposite were mixed with 80 ml of 30 ppm colored solutions and stirred. Sampling was performed at 2, 5, 10 and 15 min. Then, the samples were centrifuged 2 times and each time for 10 min at 2500 rpm. The amount of residual color was measured by the spectrophotometer and the calculation of removal percentage is given in Eq. 1.

$$\% \text{ Removal} = \frac{C_0 - C_t}{C_0} \times 100 \quad \ldots (1)$$

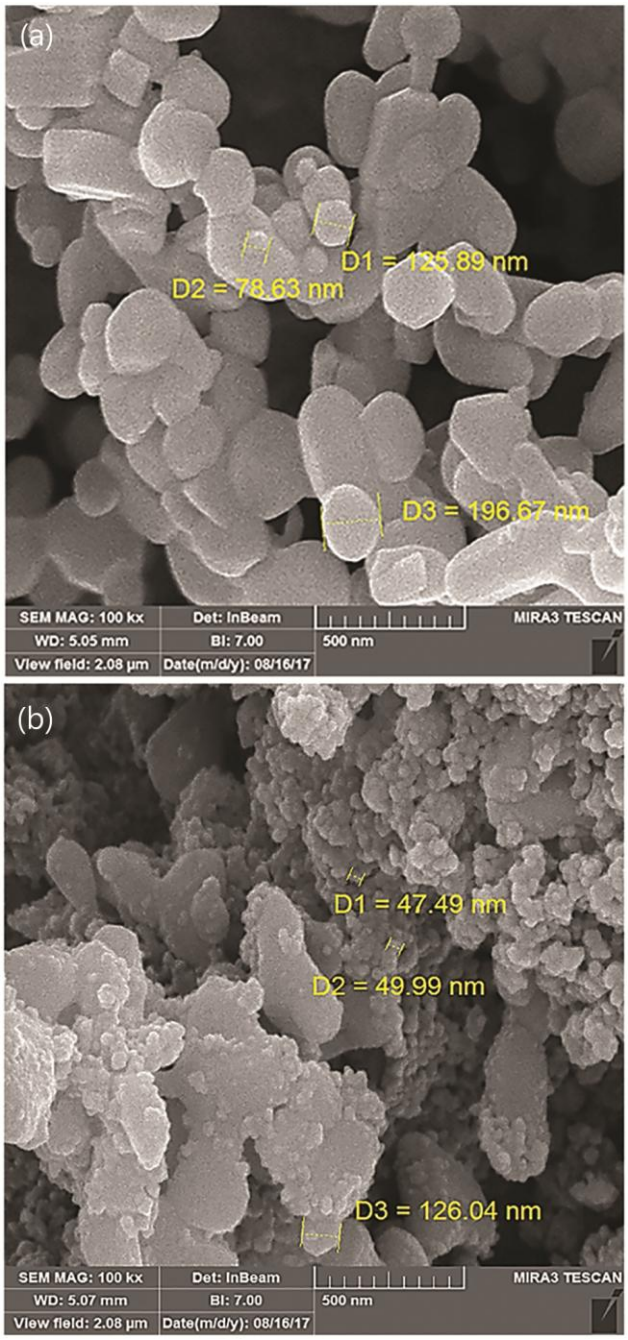

Fig. 2 — SEM of(a) $SrFe_{12}O_{19}$ and (b)$SrFe_{12}O_{19}$/nZVI

where, C_0 and C_t are the initial and the adsorbed concentration of CR, respectively. The obtained results are shown in Fig. 4 (a) and indicate that 0.12 g nanocomposite treatment has removed CR better than the other dosages. Also, 0.12 g nanocomposite treatment showed better performance in 15 min than the others. This may be because, by increasing the adsorbent dosage, increase of surface area and the active sites could occurre.

Effect of pH

Optimum dosage of nanocomposite (0.12 g) was added to three samples each of 80 ml CR solutions at pHs of 5, 8.5, and 11. The solutions were stirred and sampling was carried out after 15 min (optimal time). Each sample was centrifuged twice. The amount of residual dye was determined by the spectrophotometer and the removal efficiency was evaluated. As shown in Fig. 4 (a), the acid and alkali environments do not increase the removal percentage of the CR. Therefore, the same pH of CR (8.5) is chosen as the best pH for experiments because the best efficiency has occurred in this environment.

Effect of Dye Concentration

Three concentrations of CR tested were 20, 30, 40 mg/lit. To 80 ml of solution each, 0.12 g of nanocomposite was added, stirred, and sampled after 2, 5, 10, and 15 min. Afterward, the samples were centrifuged twice for 10 min at 2500 rpm. The residue of CR was measured and the removal efficiency was computed. As can be seen in Fig. 4 (a), the maximum removal percentage was found at 15 min with the initial concentration of 20 ppm.

Effect of Temperature

To 80 ml of 30 ppm CR solution, 0.12 g of the nanocomposite was added separately at 15, 25 and 30 °C and was stirred. Sampling was performed after 2, 5, 10, and 15 min followed by 2 times centrifugation, each time for 10 min at 2500 rpm. The value of residual color was measured and the removal efficiency was computed. As shown in Fig 4 (b), the best efficiency is related to 25°C at the optimum time of 15 min.

Study of the Adsorption Isotherms

The obtained results of adsorption of CR using Langmuir and Freundlich isotherms were studied. Langmuir equation is shown as follows:

$$C_e/q_e = (1/q_{max}.K_L) + (C_e/q_{max}) \quad \ldots (2)$$

where, q_{max} and K_L are the maximum adsorption capacity (mg/g) and the Langmuir constant (L/mg), respectively. Also, C_e and q_e are the equilibrium concentration of the CR solution (mg/L) and the

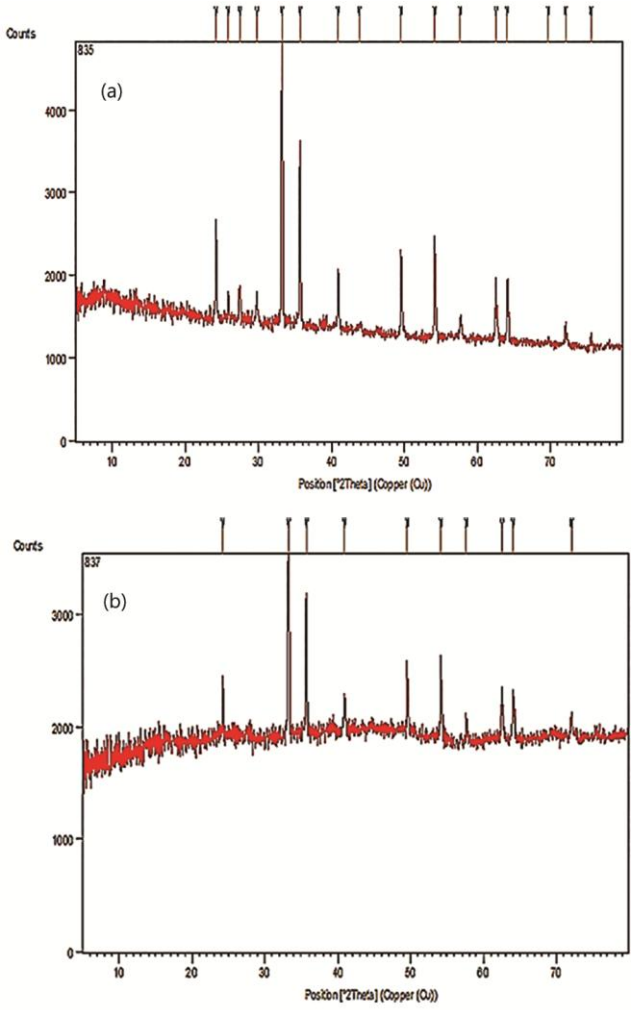

Fig. 3 — The XRD spectra of (a) doped strontium hexaferrite and (b) nanocomposite

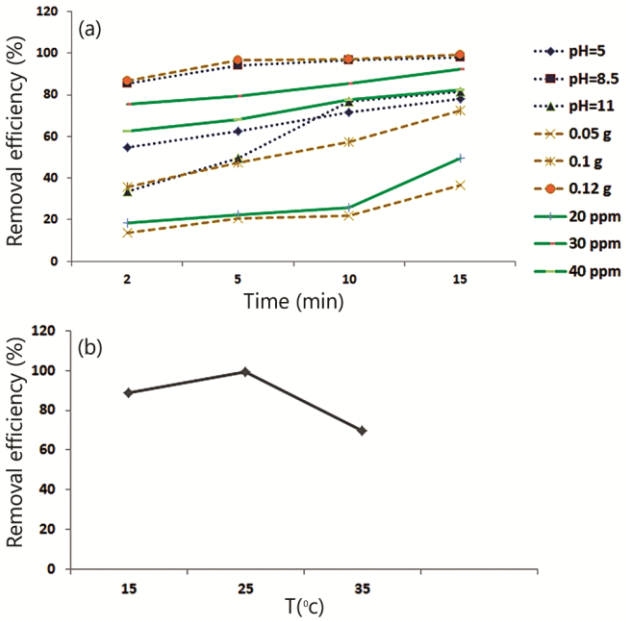

Fig. 4 — The removal efficiency of CR at (a) adsorbent dosage, different pH, different initial concentrations and (b) different temperature

amount of adsorbed dye (mg/g), respectively. Freundlich isotherm is presented in Eq. 3

$$\text{Log } q_e = \log (k_f) + \frac{1}{n} \log (C_e) \quad \ldots (3)$$

where q_e is the amount of adsorbed CR in an equilibrium condition (mg/g), k_f, n and C_e are Freundlich constant, the intensity of the adsorbent and equilibrium concentration, respectively.[36] The results are presented in Table 1. Langmuir isotherm with R^2=0.9959 shows the high capacity adsorption. It can be concluded that experimental data follow Langmuir isotherm.

Kinetic Models

To examine the rate of the adsorption process and potential rate controlling step, kinetic models are used. Pseudo-first order and pseudo-second order models are the most kinetic models. In the present study, these kinetic models were used for adsorption kinetic behavior of synthesized nanocomposite. Pseudo–first order and pseudo-second order models can be demonstrated in Eqs (4) and (5), respectively.

$$ln\,(q_e - q_t) = lnq_e - k_1(t) \quad \ldots (4)$$

$$\frac{t}{q_t} = \frac{1}{k_2 q_e^{\,2}} + \left(\frac{t}{qe}\right) \quad \ldots (5)$$

where K_1 (min^{-1}) and k_2 (g/mg/min) are the rate constant of pseudo-first order and pseudo-second order adsorption, respectively. Also, q_e and q_t are the CR adsorption capacity (mg/g) at equilibrium and time (t), respectively.[37] The calculated parameters of first order and second order kinetics are given in Table 2. The R^2 of pseudo-second order was 0.9969. Therefore, this model is suitable for the interpretation of empirical data. It shows that adsorption of dye on the $SrFe_{12}O_{19}$/nZVI adsorbent is chemical.

Study of Thermodynamic Parameters

Thermodynamic parameters such as the Gibbs free energy change (ΔG^0), entropy change (ΔS^0) and enthalpy change (ΔH^0) for adsorption of CR on $SrFe_{12}O_{19}$/nZVI can be calculated by the following equations:

$$\Delta G^0 = -RT \ln K_d \quad \ldots (6)$$

$$\ln (K_d) = \frac{\Delta S^0}{R} - \frac{\Delta H^0}{RT} \quad \ldots (7)$$

where K_d, R, and T are the distribution coefficient of adsorbent (mL/g) equal to q_e/C_e, the universal gas constant (8.314 J/mol K), the reaction temperature (K), respectively.[38] The values of ΔH^0 and ΔS^0 were estimated from the slope and intercept of the plot of ln (K_d) against 1/T and are summarized in Table 3. The positive value of ΔH^0 and ΔS^0 indicated the endothermic adsorption of CR dye.

Table 1 — The obtained parameters of isotherm models for removal of CR

Langmuir			Freundlich		
q_{max}	K_L	R^2	K_f	1/n	R^2
51.02	1.59	0.9959	5.61	0.8355	0.785

Table 2 — The obtained kinetic parameters for removal of CR

pseudo- first order			Pseudo second order		
K_1 (min^{-1})	q_e = ($mg.g^{-1}$)	R^2	K_2 ($g.mg^{-1}.\ min^{-1}$)	q_e= ($mg.g^{-1}$)	R^2
0.0741	7.500	0.8753	0.014	15.36	0.9969

Table 3 — Thermodynamic parameters for adsorption of CR

ΔH^0 (kJ/mol)	ΔS^0 (kJ/ mol K)	ΔG^0 (kJ/mol)		
		Temperature (K)		
190.44	0.650	288	298	308
		0.476	−9.355	−11.222

Conclusions

$SrFe_{12}O_{19}$/nZVI was utilized as an efficient adsorbent for the rapid treatment of CR from aqueous solution. The effect of various parameters such as pH, initial dye concentration, contact time, adsorbent weight, and temperature on the removal of CR was investigated. The isotherms and kinetic studies were investigated and the results revealed that the Langmuir and pseudo-second order were best described by the high correlation value of 0.9959 and 0.9969 respectively. Thermodynamic analysis (ΔS^0 and ΔH^0) represented that adsorption of CR onto $SrFe_{12}O_{19}$/nZVI is thermodynamically possible and endothermic. Also, Gibbs free energy change is spontaneous in 298 and 308 k. This study indicated that the synthesized nanocomposite could be a low-cost, rapid reaction, efficient, and environmentally friendly adsorbent, for removing dye from aqueous media. It can be assumed that its efficiency can depend on the degradation reaction and adsorption of pollutants resulting in the radical hydrogen being produced and the elimination of pollutants.

References

1 Yokwana K, Kuvarega A T, Mhlanga S D & Nxumalo E N, Mechanistic aspects for the removal of Congo red dye from aqueous media through adsorption over N-doped graphene

oxide nanoadsorbents prepared from graphite flakes and powders, *Phys Chem Earth*, Parts A/B/C **107** (2018) 58–70.
2 Zhang J, Yan X, Hu M, Hu X & Zhou M, Adsorption of congo red from aqueous solution using ZnO-modified SiO_2 nanospheres with rough surfaces, *J Mol Liq*, **249** (2018) 772–778.
3 Purkait M K, Maiti A, Das Gupta S & De S, Removal of congo red using activated carbon and its regeneration, *J Hazard Mater*, **145** (2007) 287–295.
4 Chen Y Y, Yu S H, Jiang H F, Yao Q Z, Fu S Q & Zhou G T, Performance and mechanism of simultaneous removal of Cd(II) and Congo red from aqueous solution by hierarchical vaterite spherulites, *Appl Surf Sci*, **444** (2018) 224–234.
5 Mahmoud M E, Abdou E H, Shehata A K, Header H M A & Hamed E A, Sustainable super fast adsorptive removal of Congo red dye from water by a novel technique based on microwave-enforced sorption process, *J Ind Eng Chem*, **57** (2018) 28–36.
6 Hu Z, Chen H, Ji F & Yuan S, Removal of congo red from aqueous solution by cattail root, *J Hazard Mater* **173** (2010) 292–297.
7 Naseem K, Farooqi Z H, Begum R & Irfan A, Removal of Congo red dye from aqueous medium by its catalytic reduction using sodium borohydride in the presence of various inorganic nano-catalysts: A review, *J Clean Prod*, **187** (2018) 296–307.
8 Satheesh R, Vignesh K, Rajarajan M, Suganthi A, Sreekantan S, Kang M & Sub Kwak B, Removal of congo red from water using quercetin modified a-Fe_2O_3 nanoparticles as effective nanoadsorbent, *Mater Chem Phys*, **180** (2016) 53–65.
9 Debnath S, Maity A & Pillay K, Impact of process parameters on removal of Congo red by graphene oxide from aqueous solution, *J Environ Chem Eng* **2** (2014) 260–272.
10 Zhang Y, Bai L, Zhou W, Lu R, Gao H & Zhang S, Superior adsorption capacity of Fe_3O_4@nSiO_2@mSiO_2 core-shell microspheres for removal of congo red from aqueous solution, *J Mol Liq* **219** (2016) 88–94.
11 Morshedi D, Mohammadi Z, M M A Boojar & Aliakbaria F, Using protein nanofibrils to remove azo dyes from aqueous solution by the coagulation process, *Colloids Surf B*, **112** (2013) 245–254.
12 Kono H & Kusumoto R, Removal of anionic dyes in aqueous solution by flocculation with cellulose ampholytes, *J Water Process Eng* **7** (2015) 83–93.
13 Al-Nakib N M H, Reverse osmosis polyamide membrane for the removal of blue and yellow dye from waste water, *Iraqi J Chem Pet Eng*, **14** (2013) 49–55.
14 Sachdeva S & Kumar A, Preparation of nanoporous composite carbon membrane for separation of rhodamine B dye, *J Membr Sci* **329** (2009) 2–10.
15 Orts F, del Rio A I, Molina J, Bonastre J & Cases F, Electrochemical treatment of real textile wastewater: Trichromy Procion HEXL®, *J Electroanal Chem* **808** (2018) 387–394.
16 Gupta V K, Jain R, Mittal A, Mathur M & Sikarwar S, Photochemical degradation of the hazardous dye Safranin-T using TiO_2 catalyst, *J Colloid Interf Sci*, **309** (2007) 464–345.
17 Venkatesh S, Venkatesh K & Rahman Q A, Dye decomposition by combined ozonation and anaerobic treatment: Cost effective technology *J Appl Res Technol* **15** (2017) 340–345.
18 Banerjee P, Das Gupta S & De S, Removal of dye from aqueous solution using a combination of advanced oxidation process and nanofiltration, *J Hazard Mater*, **140** (2007) 95–103.
19 Nayara T, de Souza V, Maria Leao de Carvalho S, Gurgel Adeodato Vieira M, Gurgel Carlos da Silva M & do Socorro Barros Brasil D, Adsorption of basic dyes onto activated carbon: Experimental and theoretical investigation of chemical reactivity of basic dyes using DFT-based descriptors, *Appl Surf Sci*, **448** (2018) 662–670.
20 Zare K, Sadegh H, Shahryari-ghoshekandi R, Maazinejad B, Ali V, Tyagi I, Agarwal S & Gupta V K, Enhanced removal of toxic Congo red dye using multi walled carbon nanotubes: Kinetic, equilibrium studies and its comparison with other adsorbents, *J Mol Liq*, **212** (2015) 266–271.
21 Tian C, Feng C, Wei M & Wu Y, Enhanced adsorption of anionic toxic contaminant Congo Red by activated carbon with electropositive amine modification, *Chemosphere* **208** (2018) 476–483.
22 Max Dias Ferreira G, Max Dias Ferreira G, Hespanhol M C, de Paula Rezende J, Clarissa S Pires A, Vinícius Alves Gurgel L & da Silva L H M Adsorption of red azo dyes on multi-walled carbon nanotubes and activated carbon: A thermodynamic study, *Collid Surf A-Physicochem Eng Asp*, **529** (2017) 531–540.
23 Liu S, Ding Y, Li P,Diao K, Tan X, Lei F, Zhan Y, Li Q, Huang B & Huang Z, Adsorption of the anionic dye Congo red from aqueous solution onto natural zeolites modified with N, N-dimethyl dehydroabietylamine oxide, *Chem Eng J*, **248** (2014) 135–144.
24 Wu Z, Yuana X, Zhong H, Wang H, Jiang L, Zeng G, Wang H, Liu Zm & Li Y, Highly efficient adsorption of Congo red in single and binary water with cationic dyes by reduced graphene oxide decorated NH_2-MIL-68 (Al), *J Mol Liq*, **247** (2017) 215–229.
25 Alver E, Bulut M, Ulku Metin A & Ciftci H, One step effective removal of Congo red in chitosan nanoparticles by encapsulation, *Spectrochim Acta A Mol Biomol Spectrosc*, 171 (2017) 132–138.
26 Ait Ahsaine H, El Jaouhari A, Bakiz B, Bazzaoui M, Albourine A & Benlhachemi A, Congo red removal by PANi/Bi_2WO_6 nanocomposites: Kinetic, equilibrium and thermodynamic studies, *J Environ Chem Eng*, **4** (2016) 3096–3105.
27 Yilmaz Ozmen E & Yilmaz M, Use of β-cyclodextrin and starch based polymers for sorption of Congo red from aqueous solutions, *J Hazard Mater*, **148** (2007) 303–310.
28 Ruikar D V, Kashid P B, Patil V R & Puri V, Synthesis, characterization and microwave properties of strontium hexaferrite thin films prepared by chemical bath deposition, *Appl Surf Sci*, 265 (2013) 475–479.
29 Wang H Z, Hai Y N, Yao B, Xu Y, Shan L, Tang J L & Wang Q H, Tailoring structure and magnetic characteristics of strontium hexaferrite via Al doping engineering, *J Magn Magn Mater*, **422** (2017) 204–208.
30 Shi L, Chen J, Wang Q & Song X, Effects of carrier on the transport and DDT removal performance of nano-zero valent iron in packed sands, *Chemosphere* **209** (2018) 489–495.
31 Zhang Q, Zhao D, Feng Sh, Wang Y, Jin J, Alsaedi A, Hayat T & Chen C, Synthesis of nanoscale zero-valent iron loaded chitosan for synergistically enhanced removal of

U(VI) based on adsorption and reduction, *J Colloid Interface Sci*, **552** (2019) 735–743.

32 Hui Diao Z, Rong Xu X & Jiang D, Bentonite-supported nanoscale zero-valent iron/persulfate system for the simultaneous removal of Cr(VI) and phenol from aqueous solutions, *Chem Eng J*, **302** (2016) 213–222.

33 Xing M, Xu L & Wang J, Mechanism of Co (II) adsorption by zero valent iron/grapheme nanocomposite, *J Hazard Mater* 301 (2016) 286–296.

34 Shi L, Zhang X & Chen Z, Removal of Chromium (VI) from wastewater using bentonite-supported nanoscale zero-valent iron, *Water Res* **45** (2011) 886–892.

35 Liu T, Zhao L, Sun D & Tan X, Entrapment of nanoscale zero-valent iron in chitosan beads for hexavalent chromium removal from wastewater, *J Hazard Mater* **184** (2010) 724–730.

36 Lui H, Rai B K, Mishra S R, Nguyen V V & Liu J P, Physical and magnetic properties of highly aluminum doped strontium ferrite nanoparticles prepared by auto-combustion route, *J Magn Magn Mater*, **324** (2012) 2602–2608.

37 Panahi H A, Rabbanib M, Zabarjad-Shiraz N, Mofavvaz S, Moniri E, Kanghari S, Entezari M & Hasanzadeh A, Synthesis and application of 5-amino-2-benzotriazol-2-yl-phenol for pre-concentration and determination of zinc (II) in water samples by flame atomic absorption spectrometry, *Desalin Water Treat*, **22** (2010) 330–339.

38 Wang Q, Tang A, Zhong L, Wen X, Yan P & Wang J, Amino-modified γ-Fe2O3/sepiolite composite with rod-like morphology for magnetic separation removal of Congo red dye from aqueous solution, *Powder Technol*, 339 (2018) 872–881.

39 Zahir A, Aslam Z, Kamal M S, Ahmad W, Abbas A & Shawabkeh R A, Development of novel cross-linked chitosan for the removal of anionic Congo red dye, *J Mol Liq*, 244 (2017) 211–218.